International Journal of Biological Macromolecules 107 (2018) 1999–2007

Contents lists available at ScienceDirect

International Journal of Biological Macromolecules

journal homepage: www.elsevier.com/locate/ijbiomac

Biochemical and biophysical characterization of a mycoredoxin protein glutaredoxin A1 from *Corynebacterium pseudotuberculosis*

Raphael J. Eberle[a], Liege A. Kawai[a], Fabio R. de Moraes[a], Ljubica Tasic[b], Raghuvir K. Arni[a], Monika A. Coronado[a,*]

[a] *Multiuser Center for Biomolecular Innovation, Departament of Physics, Instituto de Biociências Letras e Ciências Exatas (Ibilce), Universidade Estadual Paulista (UNESP), São Jose do Rio Preto, SP, 15054-000, Brazil*
[b] *Institute of Chemistry, University of Campinas (UNICAMP), Campinas, SP, 13083-970, Brazil*

ARTICLE INFO

Article history:
Received 25 July 2017
Received in revised form 6 October 2017
Accepted 11 October 2017
Available online 16 October 2017

Keywords:
Corynebacterium pseudotuberculosis
Glutaredoxin
NMR
CD spectroscopy
Inhibitors

ABSTRACT

Glutaredoxin A1 from *Corynebacterium pseudotuberculosis* was shown to be a mycoredoxin protein. In this study, we established a process to overexpress and purify glutaredoxin A1. The aim of this study was the investigation of the Glutaredoxin A1 from *C. pseudotuberculosis* behavior under different redox environments and the identification of lead molecules, which can be used for specific inhibitor development for this protein family. A quantitative assay was performed measuring the rate of insulin reduction spectrophotometrically at 640 nm through turbidity formation from the precipitation of the free insulin. Glutaredoxin A1, at 5 μM concentration, accelerated the reduction process of 0.2 mM insulin and 1 mM DTT. The pH optimum of the reaction was 7.4. In the presence of DTT and ESH the glutaredoxin A1 presents similar activity, and its activity is reduced by 50% in the presence of GSH. Additional function for ESH in the redox metabolism of *C. pseudotuberculosis* is suggested. A combined STD and Chemical Shift – NMR approach was employed to study the effects of potential inhibitors on the structure of glutaredoxin A1 from *Corynebacterium pseudotuberculosis*. The inhibitory potential of four ligands (heparin, suramin, hesperetin – Hst, and hesperidin - Hsp) against glutaredoxin A1 is discussed.

1. Introduction

C. pseudotuberculosis is a member of the heterogeneous CMNR-group of pathogens, which forms a cluster of Gram-positive bacteria along with the *Mycobacterium*, *Nocardia*, and *Rhodococcus* genus [1]. *C. pseudotuberculosis* is the causative agent of caseous lymphadenitis (CLA) that infects sheep, goats, equids (ulcerative lymphangitis) and cattle (cutaneous excoriated granulomas). CLA infection leads to dramatically reduced yields of wool and milk, weight loss, carcass condemnation and, eventually, results in death and considerable economic loss worldwide [2,3]. Rare cases of infection have also been reported in humans [4]. As a facultative intracellular parasite, this bacterium is capable of survival and growth in macrophages, thus, being able to evade detection by host immune systems [5]. There has, therefore, a strong focus on vaccination and drug development in the fight against CLA.

Controlling redox metabolism is one of the most promising approaches for drug design since it is of primary importance in rapidly growing pathogens such as *C. pseudotuberculosis.* Low molecular weight (LMW) thiols, such as glutathione (GSH), mycothiol (MSH) in mycobacteria, coenzyme-A (CoASH) in *Staphylococcus aureus* and γ-glutamylcysteine in halobacteria, play key roles in maintaining a reducing intracellular environment, which is crucial for the proper functioning of regular metabolic activities [6,7]. Thus, thiols enable rapid adaptation of microorganisms to different environmental conditions and various endogenous and exogenous stresses [8].

In eukaryotes and Gram-negative bacteria, the tripeptide glutathione (GSH) is the dominant LMW thiol [8,9]. GSH is usually present in high intracellular concentrations (approximately 5 mmol L^{-1} in *Escherichia coli*, for example), primarily in its reduced form, functioning as a thiol-disulfide redox buffer [10]. However,

Abbreviation: CLA, caseous lymphadenitis; CD, circular dichroism; CoASH, coenzyme-A; DTT, dithiothreitol; ESH, ergothioneine; Grx, glutaredoxin; GSH, glutathione; Hst, hesperetin; Hsp, hesperidin; LMW thiol, low-molecular weight thiol; Mrx, Mycoredoxin; MSH, mycothiol; Trx, thioredoxin.

* Corresponding author at: Centro Multiusuário de Inovação Biomolecular, Departamento de Física, Instituto de Biociências Letras e Ciências Exatas (Ibilce), Universidade Estadual Paulista (UNESP), Rua Cristóvão Colombo 2265, São Jose do Rio Preto, SP, 15054-000, Brazil.

E-mail addresses: eberleraphael@gmail.com (R.J. Eberle), liegekawai@gmail.com (L.A. Kawai), fabiom@ibilce.unesp.br (F.R. de Moraes), ljubica@iqm.unicamp.br (L. Tasic), arni@sjrp.unesp.br (R.K. Arni), monikacoronado@gmail.com (M.A. Coronado).

https://doi.org/10.1016/j.ijbiomac.2017.10.063
0141-8130/

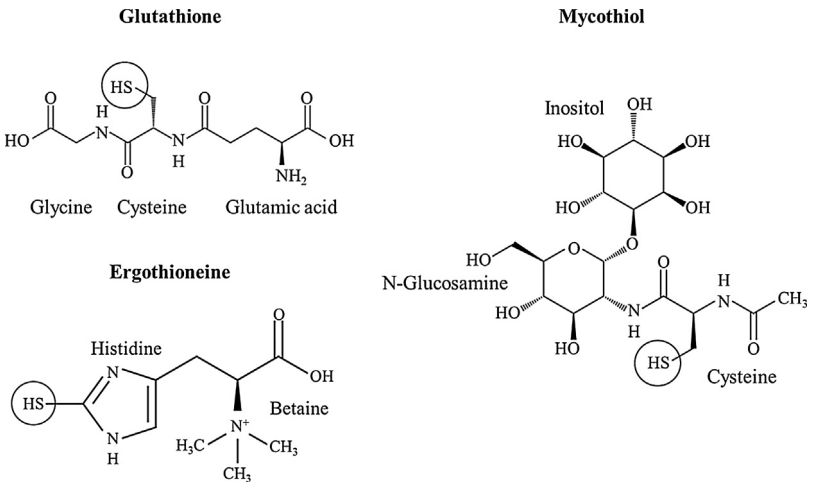

Fig. 1. Molecular structures of LMW thiols: glutathione, ergothioneine and mycothiol. Circles indicate the thiol groups.

most Gram-positive bacteria do not possess GSH, instead, the actinomycetes (*e.g.* mycobacteria, corynebacteria, and streptomyces) produce mycothiol (MSH) which is functionally analogous to GSH, as the main low-molecular weight thiol [11,12]. GSH acts not only during the regulation of oxidative stress, but also in the presence of alkylating agents and antibiotics, thereby, maintaining and regulating intracellular thiol-disulfide homeostasis [13–15]. Similar to GSH, MSH contains a functional cysteine moiety but, *myo*-inositol and *N*-glucosamine [8] are present instead of the two amino acids, glycine and glutamic acid as in GSH. Another thiol present in the actinomycetes family, including *Corynebacterium*, is ergothioneine (ESH), a 2-thiol-L-histidine betaine [8,16]. The concentration of ESH in actinomycetes is ten-fold lower than that of MSH and its exact function in these bacteria is unknown [8,17]. Beside the important thiol group in the LMW thiols their molecular structures are very different as shown in Fig. 1 for GSH, MSH and ESH.

In addition to LMW thiols, many organisms possess thiol-disulfide oxidoreductases such as thioredoxin, glutaredoxin 1, glutaredoxin 2, and glutaredoxin 3 that may function as reducing agents on protein disulfide bonds *via* their redox-active disulfides. Reduced active site thiols is essential for the catalysis of this protein. The oxidation of the cysteines inactivate the protein [18,19].

Glutaredoxins (Grx) are low molecular oxidoreductases (9–12 kDa) with a basic motif consisting of a central four-stranded anti-parallel β-sheet surrounded by three α-helices and are structurally classified as proteins with a Trx fold [20,21]. The active sites of Grx proteins (CxxC) and the glutathione binding site GGxxD motifs are conserved [20,22]. Glutaredoxins, utilize the reducing power of glutathione to catalyze disulfide reductions in the presence of NAD(P)H and glutathione reductase [20]. Grx proteins, similar to thioredoxins, participate in numerous cellular functions such as in the formation of deoxyribonucleotides for DNA synthesis (by reducing the essential enzyme ribonucleotide reductase), the generation of reduced sulfur (*via* 3′-phosphoadenylylsulfate reductase), signal transduction, and in defense against oxidative stress [19]. Grx proteins are essential for a wide spectrum of organisms and the improper functioning of this system can be correlated with various cellular dysfunctions.

In this study, we present the mechanism of the glutaredoxin A1 from *C. pseudotuberculosis* as mycoredoxin, a small protein unique to actinomycetes. LMW thiols, that could reduce *Cp*-GrxA1 was the focus of our study. The LMW thiols were tested for their reductive capacity against *Cp*-GrxA1. The specificity of glutaredoxins is not determined by the CxxC active site; moreover, other amino acids in the contact area are important [23]. Blocking the contact area maybe will disturb the substrate interaction.

Inhibition of the protein can result in a number of bacterial physiological effects. Identification of ligands, which inhibit the protein activity and can be useful as lead compounds for forward drugs development, was the second aim of this study. The inhibitory effect of four molecules was identified by enzymatic assay, and further evaluated by NMR-based techniques.

Agricultural business is suffering economic losses due to the reduction of meat, milk, and wool production, caused by CLA. Up to date there is no effective treatment for the diseases, to control the illness it is recommended that infected animals should be euthanized [2]. Vaccination has been a strategy for the prevention of CLA, but up to now vaccines are not available. It is remarkable that the understanding of the biological mechanism of the bacteria will help to the better development of an effective drug.

2. Material and methods

2.1. Materials

Diamide, dithiothreitol, coenzyme-A, ergothioneine, glutathione, low molecular weight heparin (MW: 6000 kDa), suramin, hesperetin, kanamycin, IPTG, $MgSO_4$, NaCl, Tris-HCl, glycerol, lysozyme, imidazole, K_2HPO_4, KH_2PO_4, EDTA, methanol, D2O, 4,4-dimethyl-4-silapentane-1-sulfonic acid, dmso, acetic acid and isopropanol were purchased from Sigma-Alldrich (USA). Human insulin were purchased from Eli Lilly do Brasil (Brazil). Hesperidin was produced and purified as described in Section 2.6

2.2. In silico *analysis*

Multiple Grx sequences were retrieved from NCBI and sequence alignments were performed, using MUSCLE [24] and Box Shade (http://www.ch.embnet.org/software/BOX_form.htm) web servers. The atomic coordinates from reduced *M. tuberculosis* Mrx1 (PDB: 2LQO) and oxidized *M. tuberculosis* Mrx1 (PDB: 2LQQ) were used as templates for comparative modeling by the satisfaction of spatial restraints as implemented in the program Modeller 9v13 [25]. The structure of reduced and oxidized *C. pseudotuberculosis* glutaredoxin A1 (*Cp*-GrxA1) (Gene ID: 12299035; Uniprot: D9Q987) was modeled.

2.3. Expression and purification of GrxA1

The open reading frame of *Cp*-GrxA1 was cloned into vector pD441-SR by DNA 2.0 (USA). The construct contained a N-terminal hexahistidine affinity tag. The kanamycin-resistant vector pD441-SR presents a T5 promoter inducible by IPTG and a high copy percentage provided by pUC origin of replication. Grx-pD441-SR (DNA 2.0) vectors were transformed into *E. coli* BL21 (DE3)T1 (Sigma-Aldrich, USA) competent cells, which were grown for 16 h (overnight) at 37 °C in LB medium containing sufficient amounts of kanamycin. Next, the bacterial cultures were transferred into fresh LB medium, grown for another 2.5 h at 37 °C until the A_{600} reached 0.6. Then, *Cp*-GrxA1 was induced by 0.5 mmol L^{-1} IPTG, and incubated for 4 h at 37 °C, being supplemented with 50 μmol L^{-1} $MgSO_4$. Later, the culture was harvested by centrifugation at 4000 g, 5 °C for 20 min, discarding the supernatant and re-suspending the *Cp*-GrxA1 cell pellet in 20 mmol L^{-1} Tris-HCl, pH 8.0, 500 mmol L^{-1} NaCl, 5% (v/v) glycerol. Then, the cell-suspension was incubated on ice for 1 h with lysozyme, subsequently being lysed by sonication in four sets of 30 s pulses of 30% amplitude, with 10 s intervals. This way obtained crude cell extract was centrifuged at 8000 g, 6 °C for 90 min. The supernatant containing *Cp*-GrxA1 was loaded onto Ni-NTA column pre-equilibrated with 20 mmol L^{-1} Tris-HCl, pH 8.0, 500 mmol L^{-1} NaCl, 5% (v/v) glycerol, extensively washed with the same buffer containing 20 and 40 mmol L^{-1} imidazole, *Cp*-GrxA1 eluted stepwise with 80 – 500 mmol L^{-1} imidazole. The eluted fractions were individually pooled, and injected onto a Superdex 75 10/300 GL size exclusion column (GE Healthcare), pre-equilibrated with buffer 20 mmol L^{-1} K_2HPO_4/KH_2PO_4 pH 7.4, 150 mmol L^{-1} NaCl. Sample purity after each purification step was assessed by 20% SDS-PAGE gels. Fractions containing *Cp*-GrxA1 were pooled and concentrated in a micro concentrator (MWCO: 3000 Da, GE Healthcare). Protein concentrations were determined spectrophotometrically, applying the Lambert-Beer law [26].

2.4. Circular dichroism spectroscopy (CD)

For all CD measurements, 15 repeated scans were performed, with 5 of them used to establish the baseline. The wavelength range applied for far-UV spectra was from 200 nm to 260 nm, in a time constant of 1 s and 100 nm/min continuous scanning mode, using a Jasco J-107 spectropolarimeter (Jasco, Japan). *Cp*-GrxA1 was separately diluted in 20 mmol L^{-1} K_2HPO_4/KH_2PO_4 to a concentration of 10 μmol L^{-1}. pH, from 7.0 to 9.0, were used for evaluating the secondary structure features change of *Cp*-GrxA1. Then, 10 μmol L^{-1} *Cp*-GrxA1 in 20 mmol L^{-1} K_2HPO_4/KH_2PO_4 pH 7.4 was used to investigate the influence of 1.4 μmol L^{-1} DTT, diamide, GSH, CoASH, ESH on the target protein secondary structure. In addition, 0.14 μmol L^{-1} of the ligands heparin, suramin, Hsp and Hst were individually tested with 10 μmol L^{-1} *Cp*-GrxA1. These agents and ligands were incubated with the protein for 2 h prior to the measurements. The results are presented in molar ellipticity [θ], according to:

$$[\theta]_\lambda = \frac{\theta}{c * l * 10 * n}$$

in which, θ is the ellipticity measured at a given wavelength λ (deg), c is the protein concentration (mol L^{-1}), l is the cell path length (cm) and n is the number of amino acids. CDpro software package was adopted to analyze the results [27].

2.5. Nuclear magnetic resonance (NMR)

2.5.1. Saturation transfer difference by nuclear magnetic resonance (STD-NMR)

Nuclear Magnetic Resonance (NMR) spectroscopy was used in order to map *Cp*-GrxA1 interactions with its potential modulators. All experiments were performed in a Bruker AVANCE III HD spectrometer (Bruker, Germany) operating at 600 MHz for ^1H, equipped with a triple-resonance, pulsed-field, z-gradient probe. There are several different techniques using NMR for studying protein-ligand interactions [28], ranging from protein signals to ligand signals monitoring. Saturation Transfer Difference (STD) by NMR spectroscopy is a well-established technique for such purposes [29–31]. It comprises a series of 1D experiments, described as on- and off-resonance. In the on-resonance, chosen protein signals are selectively excited and saturated. It is important that ligand signals are at least 1000 Hz away from the chosen on-resonance frequency. As a reference experiment, the off-resonance is recorded using the same pulse sequence of the on-resonance experiment, but irradiating a region far from protein or ligand signals. Due to the spin diffusion, the protein may be fully saturated, including the ligand interaction site. Intermolecular nuclear Overhauser effect (NOE) in this condition transfers magnetization from the protein to the ligand atoms, reducing the ligand signal intensity when binding takes place in the fast chemical exchange regime.

For the present study, an off-resonance at 20 ppm was chosen, and the on-resonance frequencies were selected according to the ligand signals. The Bruker pulse sequence STDDIFFESGP was used for the STD-NMR spectroscopy experiments. The protein was saturated for 2 s, the recycle delay was set to 3 s and a saturation power of 35 dBW was used. To suppress the protein signal, a spin-lock filter of 30 ms was used. STD amplification factors (STD-AF) were calculated by:

$$\text{STD} - \text{AF} = \frac{I_{\text{off-resonance}} - I_{\text{on-resonance}}}{I_{\text{off-resonance}}}$$

where $I_{\text{off-resonance}}$ and $I_{\text{on-resonance}}$ are the intensity of the ligand signals in the off- and on-resonance spectra, respectively.

Hence, 400 μmol L^{-1} suramin, 400 μmol L^{-1} Hsp and 400 μmol L^{-1} Hst were tested with 20 μmol L^{-1} of *Cp*-GrxA1 diluted in 20 mmol L^{-1} K_2HPO_4/KH_2PO_4 pH 7.4, 150 mmol L^{-1} NaCl, in order to evaluate possible interactions.

2.5.2. Chemical shift mapping by NMR

Protein-ligand interaction identification by STD-NMR is limited by affinity, *i.e.*, ligands with a dissociation constants in nmol L^{-1} range do not have a STD-AF in the difference spectra, since they are not in the fast chemical exchange regimes. Nevertheless, protein chemical shifts are sensitive to binding, especially in the nitrogen dimension, as checked throughout ^{15}N-HSQC experiment [28]. Although the proteins used in this study were not labeled, it was possible to observe chemical shift change in the protein signals following heparin titration into *Cp*-GrxA1. For this, a regular excitation sculpting experiment (ZGESGP) was recorded for a varying heparin concentration (from 10 to 350 μmol L^{-1}) on 100 μmol L^{-1} *Cp*-GrxA1. Each spectrum was referenced to DSS (4,4-dimethyl-4-silapentane-1-sulfonic acid), presented in 25 μmol L^{-1} in the solution.

2.6. Turbidimetric assay of insulin disulfide reduction

The rate of insulin disulfide reduction by *Cp*-GrxA1 was monitored spectrophotometrically following the turbidity of insulin at 640 nm [32–35], using a Biomate UV–vis Spectrophotometer (Thermo Fisher Scientific, USA). The reaction mixture A contained a total volume of 500 μL, with 0.2 mmol L^{-1} insulin, 50 mmol L^{-1}

Tris-HCL, 2 mmol L^{-1} EDTA, 5 μmol L^{-1} protein, and the optimum pH for *Cp*-GrxA1 was determined by using pH at 7.0, 7.4, 7.8, 8.0, 8.4, 8.8 and 9.0. The reaction occurred at 25 °C by adding 1 mmol L^{-1} DTT. As a control, the enzymatic reduction of insulin by *C. pseudotuberculosis* Thioredoxin A1 (*Cp*-TrxA1) was used; and, the non-enzymatic reduction of insulin by DTT. In another experiment, instead of DTT, the reductive agents GSH, ESH, CoASH and the oxidant diamide, all at 1 mmol L^{-1} final concentrations, were used. As a control, the non-enzymatic reduction of insulin with 1 mmol L^{-1} of the corresponding agent was applied.

The protein was tested in the presence of the ligands heparin, suramin, Hsp and Hst, all at final concentration of 0.14 μmol L^{-1}, to evaluate a possible inhibition on the activity of these proteins. *Cp*-GrxA1 were incubated with the ligands overnight at 4 °C and next, the samples were injected onto a Superdex 75 10/300 GL (GE Healthcare) size exclusion column pre-equilibrated with 20 mM Tris-HCL pH 7.4, 150 mM NaCl, to remove exceeding ligands. The assay was performed as described before.

The experiments were performed as triplet measurement and repeated twice, each with a new purification batch of the proteins. All data points in Fig. 5 are presented as mean ± standard deviation (SD), according to the following equation.

$$S = \sqrt{\frac{1}{N-1}\sum_{i=1}^{N}\left(Xi - \bar{X}\right)^2}$$

2.7. Production and purification of Hesperidin(Hsp)

Oven dried (70 °C) sweet orange peels (*Citrus sinensis*) were put into the Soxhlet apparatus and were de-oiled by ethyl ether during reflux for 1.5 h. Hesperidin (Hsp) was then extracted using methanol under 3 h reflux. The methanol extract was concentrated into a syrup. Hsp was crystallized using a dilute acetic acid (6%), and pale-beige needles (crude Hsp) were obtained. The crude Hsp was dissolved in dimethylsulfoxide (DMSO) forming a syrup at 60–80 °C, then, the same amount of water was added dropwise. The suspension was left to cool and Hsp crystals were removed after centrifugation and washed with small amounts of worm water and *iso*-propanol. This way, pure hesperidin was obtained and had its structure checked by NMR [36].

3. Results and discussion

3.1. Sequence analysis and molecular modeling of cp-GrxA1

A BLAST search for the *Cp*-GrxA1 sequence against the non-redundant protein sequences database [37] indicated that the protein sequence is highly conserved within the *Corynebacterium* genus with an identity of approximately 88% (*C. ulcerans*). On the other hand, the identity with the *E. coli* Grx1 sequence was less than 10% (Fig. 2A). The active site dithiol motif (CxxC) is conserved across the Grx/Trx protein family. The *E. coli* Grx1 sequence contains a GGxxD motif considered to be important for interaction with GSH [20,22] which is absent in *Cp*-GrxA1 since *C. pseudotuberculosis* utilizes MSH [38,13].

Although GSH and MSH are functionally similar [15,39], they are structurally very different; GSH is a tripeptide, whereas; MSH carries the saccharides, *N*-glucosamine, *myo*-inositol and a cysteine moiety [40]. The *Cp*-GrxA1 sequence shares low sequence identity with other Grx proteins, but, it shares significant sequence identity with the mycoredoxin proteins (Fig. 2B).

The two motifs VPT and TNP in the Mrx1 of *M. tuberculosis* are located in the region where it can be implicated in recognition of the glucosamine inositol (GlcN-Ins) portion of MSH [15]. These motifs are conserved within the Mrx proteins and *Cp*-GrxA1 (Fig. 2A and B). However, the aforementioned GGxxD motif, important for interaction with GSH, is absent, indicating that *Cp*-GrxA1 could function as a Mrx protein. Grx proteins contain a conserved *cis*-proline, which is implicated in stabilization of the active site and which also participates in catalysis [41,42].

Generally, Grx proteins, for example *E. coli* Grx, contain the CxxC motif without the presence of the adjacent Trp residue, which is conserved in Trx proteins [20,43]. Interestingly, the Mrx sequences presented in Fig. 2B contain this Trp residue. The importance of this amino acid in the *E. coli* Trx active site has been examined [44] and mutations decrease disulfide reduction by about 50%.

A *Cp*-GrxA1 homology model was generated based on the structure of the *M. tuberculosis* Mrx1 (PDB: 2LQO; sequence identity of 46% and a sequence coverage of 97%). Results of the comparisons of the *Cp*-GrxA1 homology model, with the *M. tuberculosis* Mrx1 and the *E. coli* Grx1 (PDB: 1EGR) structures is presented in Fig. 3A.

The three proteins possess the typical fold, which is conserved across different bacterial species, consisting of a central twisted four-stranded anti-parallel central β-sheet flanked on three sides by α-helices [21]. α-helix one and the four β-strands are in the same relative orientations in the three structures. α-helices two and three present significant differences in Mrx and Grx, which can be correlated with the variation in the molecular structure of the substrates as indicated previously in Fig. 1. The mycoredoxin proteins contain a long linker peptide between β-strand four and α-helix three and in the *E. coli* Grx structure this loop is truncated. The dithiol active site of those proteins is conserved (Fig. 3B) and is located in α-helix one and the following loop connection with β-sheet one.

The VPT and TNP motifs in *Cp*-GrxA1 and *M. tuberculosis* Mrx1 are located in the same region of the proteins and structural overlays of these motifs indicate structural conservation (Fig. 3C). The VPT motif is located in the loop connecting α-helix two and β-sheet three and the TNP motif in the loop connecting β-sheet four and α-helix three, both motifs are located near the active site.

A structural comparison between the *Cp*-GrxA1 model and the *E. coli* Grx1 protein structure indicates that the TNP and the GGxxD motifs overlap in their positions (Fig. 3D). The location of the TNP and VPT motifs in *Cp*-GrxA1 is similar to the position of GGxxD motif in the *E. coli* Grx1, indicating the participation of this region in the MSH binding [15].

3.2. Expression and purification

99 amino acids comprise the protein sequence of *Cp*-GrxA1 with a molecular weight of ~11,155.3 Da. Cloning, expression and purification protocols are described in detail in item 2.2 of this article. The protein presented a single band on a SDS-PAGE gel following size exclusion chromatography (Fig. S1, Supplementary material) with a mass of approximately 11 kDa.

3.3. Insulin reduction by cp-GrxA1

To test the general *Cp*-GrxA1 thiol-disulfide oxidoreductase activity, a classical insulin reduction assay was performed. In this assay, the putative redox-active proteins reducing insulin disulfide bonds and the subsequent precipitation of insulin was followed turbidimetrically at 640 nm [32–35]. Two control experiments where performed, the first one without *Cp*-GrxA1 and no precipitation was observed up to 20 min. The second control experiment was realized with Thioredoxin A1 from *C. pseudotuberculosis* (*Cp*-TrxA1), which was prepared in our lab.

The general thiol-disulfide oxidoreductase activity of both proteins tested indicates significant differences. *Cp*-TrxA1 reaches a

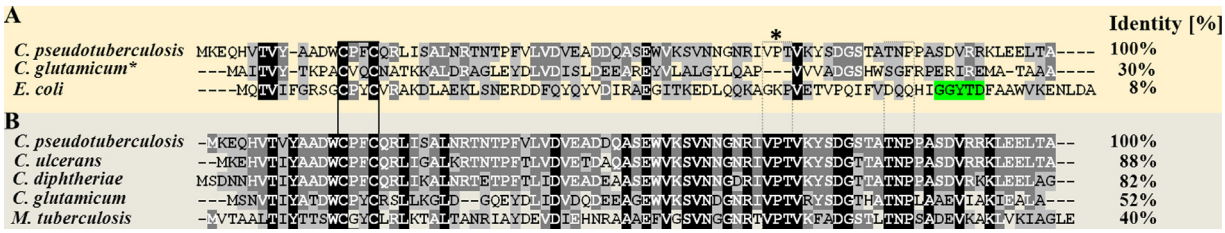

Fig. 2. Sequence comparisons of bacterial Grx proteins. A: sequence alignment of *Cp*-GrxA1, *C. glutamicum* Nrdh-redoxin (marked by star), and *E. coli* Grx1. B: Sequence BLAST of *Cp*-GrxA1 against mycoredoxin from *C. ulcerans* Grx, *C. diphtheriae* Grx, *C. glutamicum* Mrx1, *M. tuberculosis* Mrx1. The dithiol active site residues (CxxC) (black box). The VPT and TNP motifs in the Mrx and Mrx-like proteins (dashed boxes). The asterisk indicates the position of the *cis*-proline. The GGxxD motif, is highlighted in green.

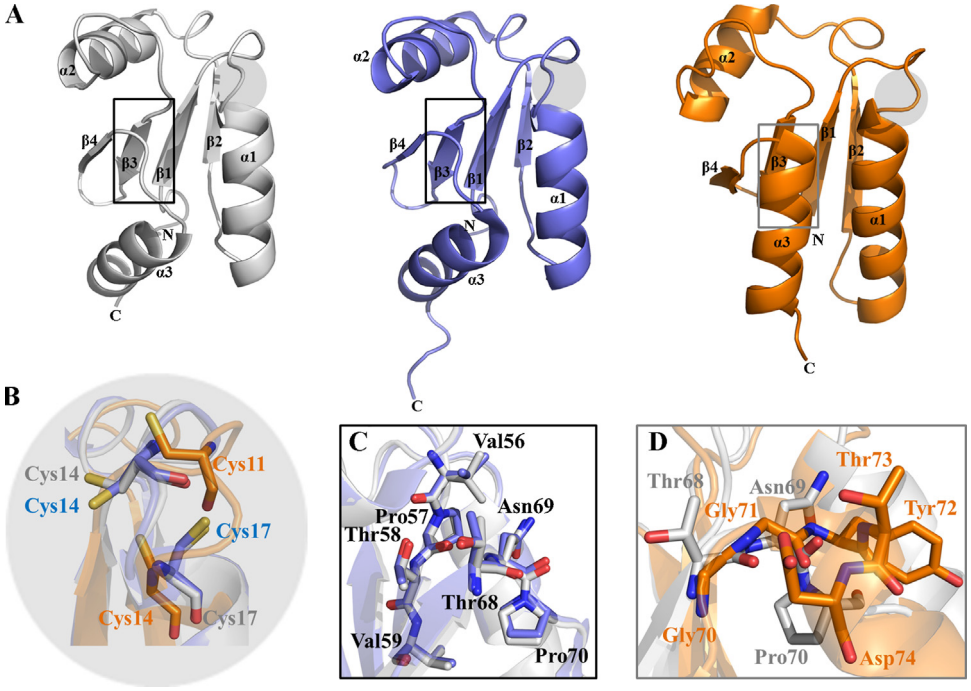

Fig. 3. Structural comparisons of the *Cp*-GrxA1 homology model with *M. tuberculosis* Mrx1 (PDB: 2LQO) and *E. coli* Grx1 (PDB: 1EGR). A: *Cp*-GrxA1(grey), *M. tuberculosis* Mrx1 (blue), and *E .coli* Grx1 (orange). The grey spheres indicate the active sites. The black boxes mark the position of the VPT and TNP motifs in the Mrx proteins. The grey box labels the position of the GGxxD motif in the *E. coli* Grx1. B: Structural overlay of the active site motif of the three proteins. C: Structural overlay of the VPT and TNP motifs in *Cp*-GrxA1 and *M. tuberculosis* Mrx1. D: Structural comparison of the *Cp*-CrxA1 TNP motif and the *E .coli* Grx1 GGxxD motif. (For interpretation of the references to colour in this figure legend, the reader is referred to the web version of this article.)

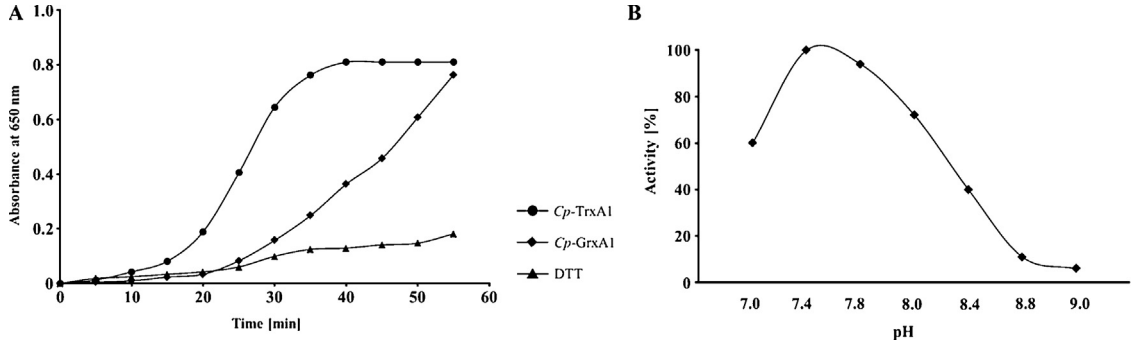

Fig. 4. Insulin reductase activity by *Cp*-GrxA1. A: Reduction of insulin by *Cp*-GrxA1. As control served *Cp*-TrxA1 and 1 mmol L^{-1} DTT. B: pH profile of *Cp*-GrxA1 using the assay of reduction of insulin in pH range from 7.0 to 9.0.

saturation level after 38 min and *Cp*-GrxA1 does not follow this pathway (Fig. 4A).

The function of thioredoxin is the reduction of oxidized cysteines in proteins with electrons obtained from NAD(P)H *via* the NAD(P)H-dependent flavoenzyme – Thioredoxin reductase pathway [45]. Insulin in this reduction assay is a typical substrate for *Cp*-TrxA1. In contrast, Grx proteins specifically reduce oxidized GSH and in the case of *Cp*-GrxA1, MSH. The differences in the substrate preference of both proteins are observable in Fig. 4A. *Cp*-GrxA1 has the potential to reduce insulin, but saturation of the catalysis is not attained. *Cp*-TrxA1 attains saturation after approximately 35 min. The evaluation of redox agents and ligands on the enzymatic reduc-

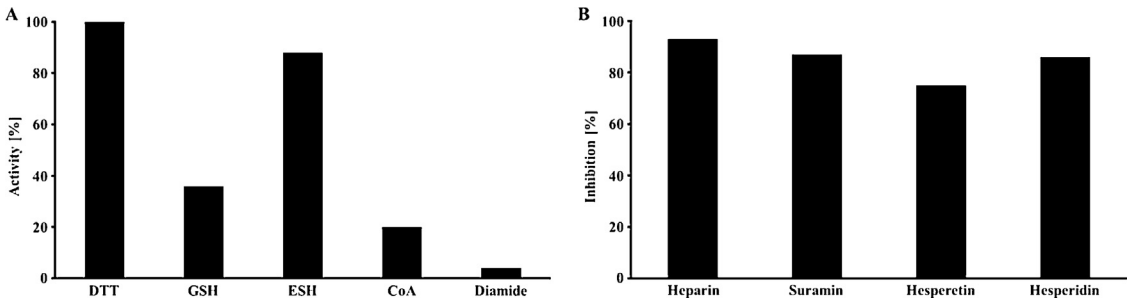

Fig. 5. Influence of redox agents and ligands on the insulin reduction by *Cp*-GrxA1. A: Activity [%] of *Cp*-GrxA1 on the reduction of insulin in the presence of DTT, GSH, ESH, CoASH, and diamide. B: Inhibition of *Cp*-GrxA1 activity [%] on the reduction of insulin in the presence of one of these ligands: heparin, suramin, hesperetin, hesperidin.

tion of insulin by *Cp*-GrxA1 were performed at pH 7.4 since the highest reductase activity is at pH 7.4 for *Cp*-GrxA1 (Fig. 4B).

Cp-GrxA1 presents a similar activity in the presence of DTT and ESH, the activity was lowered by 50% in the presence of GSH. CoASH or diamide had the lowest effect on the protein activity compared with the results in the presence of DTT (Fig. 5A).

Diamide leads to the oxidation of cysteines at the active site, rendering them unavailable to reduce insulin thereby reducing the target-enzyme activity significantly.

DTT is a relatively small molecule when compared with GSH, ESH and CoA, so that steric hindrance of the protein is unlikely to influence the reduction of the active site residues. The absence of the GGxxD motif in *Cp*-GrxA1, which is important for the interaction with GSH [20,22], may account for the low reduction capacity.

Besides DTT, ESH showed the strongest effect on the insulin reduction by *Cp*-GrxA1, which has not been described previously. The ability of ESH to reduce *Cp*-GrxA1 indicates an additional function for this compound in the redox metabolism in *C. pseudotuberculosis*. Data bank analysis of the *Corynebacterium* species genome demonstrates the presence of genes involved in the ESH synthesis, egtA, egtB, egtC, egtD and egtE.

Four ligands (heparin, suramin, hesperetin - Hst and hesperidin - Hsp), were tested for their inhibitory potentials of *Cp*-GrxA1 (Fig. 5B). The assays were performed as described above and the proteins where reduced with 1 mmol L^{-1} DTT. To overcome the effects of the free ligands on insulin, the proteins were incubated with the ligands for 16 h (overnight) and subsequently the unbound ligands were eleminated by size-exclusion chromatography. All compounds tested inhibited protein activity by greater than 80%. The greatest inhibition observed was for heparin followed by suramin, Hsp and Hst.

Heparin is a linear, polydisperse polysaccharide consisting of repeating units of $1\rightarrow4$-linked pyranosyluronic acid and 2-amino-2-deoxyglucopyranose (glucosamine) residues [46]. Heparin-binding sites in proteins are characterized by the presence of clusters of positively charged basic amino acids that form ion pairs with spatially defined negatively charged sulfo- or carboxyl groups of heparin [47]. Additionally, *Cp*-GrxA1 contains the VPT and TNP motifs which interact with the GlcN-Ins segment of MSH and the sugar moieties of heparin probably bind to this region is high.

Suramin, a symmetric divalent molecule, containing two naphthalene-trisulfonic acid head groups, is a well characterized analogue of heparin and it has be shown that both compete for the same binding region of the protein [48,49].

Hsp and Hst are citrus flavonoids that show interesting biological activities. Hsp is a flavanone glycoside and its aglycone form is Hst [50]. Some properties of these compounds include anticancer, cancer preventive, anti-inflammatory, neuroprotective and antioxidant properties, which are well-known and promising properties [51–54]. Hst is the aglyconated form of hesperidin and the disaccharide rutinose is absent, this disaccharide consists of glucose and rhamnose molecules. It is assumed that this disaccharide promotes the interaction with *Cp*-GrxA1, probably due to the presence of the VPT and TNP motifs.

3.4. Circular dichroism

CD-measurements were conducted to evaluate changes in the protein secondary structure features as a function of pH and concentration of reducing/oxidizing agents, and ligands. The results were evaluated by utilizing the CDpro software (Table S2, Supplementary material).

The secondary structure of *Cp*-GrxA1 (Fig. 6A) was sensitive to changes in pH; at pH 7.0, the α-helical and β-sheet contents were around 30% and 22% respectively. Increasing the pH to 9.0 resulted in an increase of the α-helical content to around 37% and a concomitant decrease in the β-sheet content to around 15%. This is in good agreement with the crystal structure of *M. tuberculosis* Mrx1 (PDB: 2LQO), which has α -helical and a β-sheet content of 34% and 17% respectively.

In the presence of diamide, these values changed to 40% α-helix, 14% β-sheet, 18% turn, and 28% random coil (Fig. 6B). Treatment with DTT and GSH showed a similar spectrum to the untreated protein (Fig. 6B and table S2 supplementary material). To visualize the changes in the secondary structure of the protein, homology models of reduced and oxidized *Cp*-GrxA1 were generated based on the coordinates of reduced (PDB: 2LQO) and oxidized (PDB: 2LQQ) Mrx1 from *M. tuberculosis* (Fig. S2, Supplementary material).

In the presence of CoASH, the CD spectrum of *Cp*-GrxA1 undergoes a weak signal reduction. Since the results of the insulin reduction assay also indicate a weak effect on the protein activity, we can conclude that CoASH does not have a strong influence on the protein activity or secondary structure.

Contrary to the significant changes induced by GSH and DTT, ESH presented only a slight modification of the protein CD signal probably by reducing the active site residues. The insulin reduction assay for *Cp*-Grx-A1 indicated that ESH has a strong effect however, further investigations are necessary to determine its binding mode.

The ligands, tested for their inhibitory potential in the insulin reduction assay were investigated regarding their effects on the secondary structure of the proteins, as presented in Fig. 6C. The results confirmed that the tested ligands possess no denaturation or unfolding effect on the protein. The *Cp*-GrxA1 secondary structure was influenced by Hst and Hsp in a similar fashion and showed an inverse effect compared with the suramin and heparin CD signals. Hsp binding can induce conformational changes in proteins [55,56], similar to the CD results of *Cp*-grxA1 described above.

Suramin and heparin are agonists and generally compete for the same binding sites in proteins and have a similar effect on the CD spectra of *Cp*-GrxA1 [38–40].

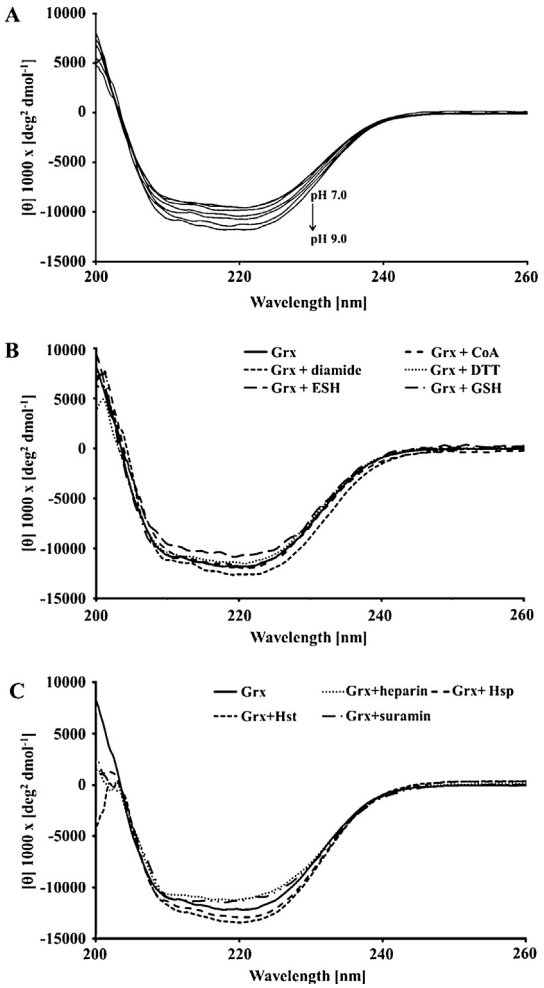

Fig. 6. Far-UV CD-spectra from 200 to 260 nm of *Cp*-GrxA1 under different conditions. A: CD-spectra of *Cp*-GrxA1 in the pH range from 7.0 to 9.0. B: CD-spectra of *Cp*-GrxA1 incubated with diamide, ESH, DTT, CoA, or GSH. C: Influence of heparin, suramin, Hsp or Hst on the CD-spectra of *Cp*-GrxA1.

3.5. Nuclear magnetic resonance (NMR)

Saturation Transfer Difference (STD) NMR experiments were performed to identify the interactions and to investigate the binding epitopes of the four inhibitors with *Cp*-GrxA1.

Evaluating the Hst binding epitopes (Fig. S3, Supplementary material) was the most challenging since all observed hydrogens were subjected to the STD effects. The highest relative STD amplification factors (STD-AF), rated with 100% and determined for the hydrogens of the aromatic ring system (Fig. S3, Supplementary material). The flavonoid Hst showed a strong inhibitory effect on the insulin reduction activity of *Cp*-GrxA1, the identification of the binding epitopes of this ligand provide useful information for docking experiments and refining possible poses, to determine the binding region of this molecule to *Cp*-GrxA1.

Cp-GrxA1 interaction with Hsp could be confirmed (Fig. S3, Supplementary material), and interestingly, the binding epitopes of Hsp and Hst indicated significant differences in their interactions with *Cp*-GrxA1. In Hsp the relative STD-AF of the CH_3 group next to the ether-bond changes from 57% to around 87%. The aromatic ring systems in Hsp are not involved in the interaction with *Cp*-GrxA1, in contrast to Hst. The CH_3 group of the rhamnose moiety of rutinose in the Hsp molecule shows the highest relative STD-AF. The disaccharide rutinose strongly affects the binding behavior of the molecule probably due to the VPT and TNP motifs which

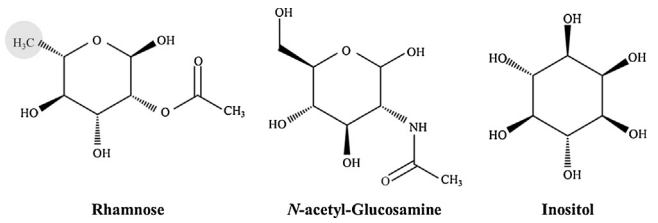

Fig. 7. Molecular structures of rhamnose (part of rutinose), *N*-acetyl-glucosamine and inositol (part of MSH). The grey sphere indicates the CH_3 group, which interacts with *Cp*-GrxA1.

can support this interaction. Compared with the sugar moieties of MSH, inositol and *N*-glucosamine, rhamnose is similar to *N*-acetyl glucosamine as illustrated in Fig. 7.

Currently, the details of the mode of interaction of MSH/Mrx is unknown, however, as mentioned earlier, the VPT and TNP motifs seem to have an impact on MSH binding by recognizing the GlcN-Ins portion of MSH [15]. Our results demonstrate that Hsp interacts with *Cp*-GrxA1 and the interaction has an influence on the active site, because of the observed inhibition of the protein in the insulin reduction assay. Based on these observations, we may conclude that Hsp binds on, or very near, to the VPT and TNP motifs. Additional experiments are necessary to confirm this and to test Hsp as a potential lead compound to generate specific *Cp*-GrxA1 inhibitors.

Binding between suramin and *Cp*-GrxA1 is induced by the aromatic rings of the compound, which receive most of the transferred magnetization as observed in the STD experiments (Fig. S4, Supplementary material).

The interaction of heparin with *Cp*-GrxA1 could not be verified using STD-NMR experiments. This is potentially due the associated affinity cut-off necessary to dissociate heparin from the protein for the measurement of the binding event. Protein-ligand complexes with dissociation constants lower than a few micromols are not observable in STD-NMR experiments. Nevertheless, using the chemical shift changes after ligand titration by NMR 1-D spectra of the protein, this interaction could be confirmed (Fig. S5, Supplementary material). Unfortunately, ligand titration could not provide information about the binding epitopes of the ligand.

4. Conclusion

Intracellular pathogens, like *C. pseudotuberculosis*, survive in very challenging environments, where the host cells attack them continuously. Notwithstanding, they still present themselves as rapidly-growing cells, with high metabolism rates. The pathogen has to deal with high amounts of cell-toxic reactive oxygen species created by these origins. A disharmony in the detoxification of these molecules can strongly influence the cellular redox homeostasis. Thus, pathogens' redox metabolism represents one of the most promising targets for drug design.

Cp-GrxA1 is a member of the Grx protein family and shows similarities in the core structure and the CxxC active site. Sequence analysis of *Cp*-GrxA1 showed that the protein contains two carbohydrate binding regions (VPT and TPN), typical for Mrx proteins. In contrast, the typical GGxxD motif for Grx is absent from the *Cp*-GrxA1, which give us a clear cue that GrxA1 from *C. pseudotuberculosis* is a Mrx-like protein.

The *Cp*-GrxA1 thiol-disulfide oxidoreductase activity on insulin showed strong effects, when the protein was reduced with DTT or ESH. The reduction of *Cp*-GrxA1 with ESH has not been reported previously and is characterized for the first time and, this result could expand the function of this LMW thiol as a back-up system for MSH in actinomycetes species.

We also describe, for the first time, the binding behaviors and inhibitory effects of suramin, heparin, hesperidin and hesperetin on *Cp*-GrxA1 using biochemical and biophysical methods. Our results can be used as basis for further experiments to identify lead compounds and design potential inhibitors for this protein family.

Conflict of interest

Authors declare that there exists no conflict of interest.

Author contributions

Raphael J. Eberle expressed and purified *Cp*-GrxA1. Liege A. Kawai expressed and purified *Cp*-TrxA1. Raphael J. Eberle performed the experimental procedures. Fabio R. de Moraes performed the NMR experiments and analyses. Ljubica Tasic purified and provided the hesperidin (Hst) and hesperetin (Hsp) flavonoids. Raghuvir K. Arni guided the research and the elaboration of the manuscript. Monika A. Coronado coordinated the research and advised the elaboration of the manuscript. All authors read and took part in revising the final manuscript version.

Aknowledgements

This research was supported by grants from CNPq [Grant numbers 435913/2016-6, 401270/2014-9, 307338/2014-2], FAPESP [Grant numbers 2015/13765-0, 2015/18868-2, 2016/08104-8; 2016/12904-0; 2009/53989-4], CAPES and PROPe UNESP.

Appendix A. Supplementary data

Supplementary data associated with this article can be found, in the online version, at https://doi.org/10.1016/j.ijbiomac.2017.10.063.

References

[1] F.A.P. Dorella, L.G. Carvalho, S.C. Oliveira, A. Miyoshi, V. Azevedo, *Corynebacterium pseudotuberculosis*: microbiology, biochemical properties, pathogenesis and molecular studies of virulence, Vet. Res. 37 (2006) 201–218.
[2] M.W. Paton, I.R. Rose, R.A. Hart, S.S. Sutherland, A.R. Mercy, T.M. Ellis, J.A. Dhaliwal, New infection with Corynebacterium pseudotuberculosis reduces wool production, Aust. Vet. J. 71 (1994) 47–49.
[3] J.L. Ayers, Caseous lymphadenitis in goats and sheep: a review of diagnosis, pathogenesis, and immunity Corynebacterium pseudotuberculosis, J. Am. Vet. Med. Assoc. 171 (1977) 1251–1254.
[4] M.M. Peel, G.G. Palmer, A.M. Stacpoole, T.G. Kerr, Human lymphadenitis due to *Corynebacterium pseudotuberculosis*: report of ten cases from Australia and review, Clin. Infect. Dis. 24 (1997) 185–191.
[5] S. Mckean, J. Davies, R. Moore, Identification of macrophage induced genes of *Corynebacterium pseudotuberculosis* by differential fluorescence induction, Microbes Infect. 7 (2005) 1352–1363.
[6] A. Gaballa, G.L. Newton, H. Antelmann, D. Parsonage, H. Upton, M. Rawat, A. Claiborne, R.C. Fahey, J.D. Helmann, Biosynthesis and functions of bacillithiol, a major low-molecular-weight thiol in Bacilli, Proc. Natl. Acad. Sci. U. S. A. 107 (2010) 6482–6486.
[7] G.L. Newton, K. Arnold, M.S. Price, C. Sherrill, S.B. Delcardayre, Y. Aharonowitz, G. Cohen, J. Davies, R.C. Fahey, C. Davis, Distribution of thiols in microorganisms: mycothiol is a major thiol in most actinomycetes, J. Bacteriol. 178 (1996) 1990–1995.
[8] M. Rawat, Y. Av-Gay, Mycothiol-dependent proteins in actinomycetes, FEMS Microbiol. Rev. 31 (2007) 278–292.
[9] M.E. Anderson, Glutathione: an overview of biosynthesis and modulation, Chem. Biol. Interact. 111 (1998) 1–14.
[10] N.S. Kosower, E.M. Kosower, The glutathione status of cells, Int. Rev. Cytol. 54 (1978) 109–160.
[11] M. Si, L. Zhang, M.T. Chaudhry, W. Ding, Y. Xu, C. Chen, A. Akbar, X. Shen, S.J. Liu, *Corynebacterium glutamicum* methionine sulfoxide reductase A uses both mycoredoxin and thioredoxin for regeneration and oxidative stress resistance, App. Environ. Microbiol. 8 (2015) 2781–2796.
[12] G.L. Newton, Y. Av-Gay, R.C. Fahey, A novel mycothiol-dependent detoxification pathway in mycobacteria involving mycothiol S-conjugate amidase, Biochemistry 39 (2000) 10739–10746.
[13] M. Rawat, G.L. Newton, M. Ko, G.J. Martinez, R.C. Fahey, Y. Av-Gay, Mycothiol-deficient *Mycobacterium smegmatis* mutants are hypersensitive to alkylating agents free radicals, and antibiotics, Antimicrob. Agents Chemother. 46 (2002) 3348–3355.
[14] N. Buchmeier, R.C. Fahey, The mshA gene encoding the glycosyltransferase of mycothiol biosynthesis is essential in *Mycobacterium tuberculosis* Erdman, FEMS Microbiol. Lett. 264 (2006) 74–79.
[15] K. Van Laer, L. Buts, N. Foloppe, D. Vertommen, K. Van Belle, K. Wahni, G. Roos, L. Nilsson, L.M. Mateos, M. Rawat, N.A.J. Van Nuland, J. Messens, Mycoredoxin-1 is one of the missing links in the oxidative stress defence mechanism of Mycobacteria, Mol. Microbiol. 86 (2012) 787–804.
[16] D.S. Genghof, Biosynthesis of ergothioneine and hercynine by fungi and Actinomycetales, J. Bacteriol. 103 (1977) 475–478.
[17] R.C. Fahey, Novel thiols of prokaryotes, Annu. Rev. Microbiol. 55 (2001) 333–356.
[18] J.F. Collet, J. Messens, Structure function, and mechanism of thioredoxin proteins, Antioxid. Redox Signal. 13 (2010) 1205–1216.
[19] W.A. Prinz, F. Åslund, A. Holmgren, J. Beckwith, The role of the thioredoxin and glutaredoxin pathways in reducing protein disulfide bonds in the *Escherichia coli* cytoplasm, J. Biol. Chem. 272 (1997) 15661–15667.
[20] C.H. Lillig, C. Berndt, Glutaredoxins in thiol/disulfide exchange, Antioxid. Redox Signal. 18 (2013) 1654–1665.
[21] J.L. Martin, Thioredoxin—a fold for all reasons, Structure 3 (1995) 245–250.
[22] C.H. Lillig, C. Berndt, A. Holmgren, Glutaredoxin systems, BBA-Gen. Subjects 1780 (2008) 1304–1317.
[23] C. Berndt, J.D. Schwenn, C.H. Lillig, The specificity of thioredoxins and glutaredoxins is determined by electrostatic and geometric complementarity, Chem. Sci. 6 (2015) 7049–7058.
[24] R.C. Edgar, MUSCLE: a multiple sequence alignment method with reduced time and space complexity, BMC Bioinf. 5 (2004) 113.
[25] N. Eswar, M.A. Marti-Renom, B. Webb, M.S. Madhusudhan, D. Eramian, M. Shen, U. Pieper, A. Sali, Comparative protein structure modeling with MODELLER, Curr. Protoc. Bioinformatics 15 (2007) 1–30.
[26] G.R. Grimsley, C.N. Pace, Spectrophotometric determination of protein concentration, Curr. Protoc. Protein Sci. 3.1 (1.9) (2004) 1–3.
[27] N. Sreerama, R.W. Woody, Computation and analysis of protein circular dichroism spectra, Methods Enzymol. 383 (2004) 318–351.
[28] M. Bieri, A.H. Kwan, M. Mobli, G.F. King, J.P. Mackay, P.R. Gooley, Macromolecular NMR spectroscopy for the non-spectroscopist: beyond macromolecular solution structure determination, FEBS J. 278 (2011) 704–715.
[29] M. Mayer, B. Meyer, Group epitope mapping by saturation transfer difference NMR to identify segments of a ligand in direct contact with a protein receptor, J. Am. Chem. Soc. 123 (2001) 6108–6117.
[30] M. Mayer, B. Meyer, Characterization of ligand binding by saturation transfer difference NMR spectroscopy, Angew. Chem. Int. Ed. Engl. 38 (1999) 1784–1788.
[31] J. Angulo, I. Díaz, J.J. Reina, G. Tabarani, F. Fieschi, J. Rojo, P.M. Nieto, Saturation transfer difference (STD) NMR spectroscopy characterization of dual binding mode of a mannose disaccharide to DC-SIGN, Chem. Bio. Chem. 9 (2008) 2225–2227.
[32] S. Rahlfs, M. Fischer, K. Becker, Plasmodium falciparum possesses a classical glutaredoxin and a second, glutaredoxin-like protein with a PICOT homology domain, J. Biol. Chem. 276 (2001) 37133–37140.
[33] H. Kurooka, K. Kato, S. Minoguchi, Y. Takahashi, J.E. Ikeda, S. Habu, N. Osawa, A.M. Buchberg, K. Moriwaki, H. Shisa, T. Honjo, Cloning and characterization of the nucleoredoxin gene that encodes a novel nuclear protein related to thioredoxin, Genomics 39 (1997) 331–339.
[34] A. Jordan, F. Åslund, E. Pontis, P. Reichard, A. Holmgren, Characterization of *escherichia coli* Nrdh a glutaredoxin-like protein with a thioredoxin-like activity profile, J. Biol. Chem. 272 (1997) 18044–18050.
[35] A. Holmgren, Glutathione-dependent synthesis of deoxyribonucleotides. Characterization of the enzymatic mechanism of *Escherichia coli* glutaredoxin, J. Biol. Chem. 254 (1979) 3672–3678.
[36] L. Tasic, B. Mandic, C.H.N. Barros, D.Z. Cypriano, D. Stanisic, L.G. Schultz, L. da Silva, M.A.M. Mariño, V.L. Queiroz, Exploring bioactivity of hesperidin, naturally occurring flavanone glycoside, isolated from oranges, in: D. Simmons (Ed.), Citrus Fruits, Nova Science Publishers, Inc., 2016 (ISBN: 978-1-63484-079-8).
[37] W. Gish, W. Miller, E.W. Myers, D.J. Lipman, Basic local alignment search tool, J. Mol. Biol. 215 (1990) 403–410.
[38] N.A. Buchmeier, G.L. Newton, R.C. Fahey, A mycothiol synthase mutant of *Mycobacterium tuberculosis* has an altered thiol-disulfide content and limited tolerance to stress, J. Bacteriol. 188 (2006) 6245–6252.
[39] M.P. Patel, J.S. Blanchard, Expression, purification, and characterization of *Mycobacterium tuberculosis* mycothione reductase, Biochemistry 38 (1999) 11827–11833.
[40] G.L. Newton, C.A. Bewley, T.J. Dwyer, R. Horn, Y. Aharonowitz, G. Cohen, J. Davies, D.J. Faulkner, R.C. Fahey, The structure of U17 isolated from *Streptomyces clavuligerus* and its properties as an antioxidant thiol, Eur. J. Biochem. 230 (1995) 821–825.
[41] C. Nathaniel, L.A. Wallace, J. Burke, H.W. Dirr, The role of an evolutionarily conserved cis-proline in the thioredoxin-like domain of human class Alpha glutathione transferase A1-1, Biochem. J. 372 (2003) 241–246.
[42] J.B. Charbonnier, P. Belin, M. Moutiez, E.A. Stura, E. Quemeneur, On the role of the cis-proline residue in the active site of DsbA, Protein Sci. 8 (1999) 96–105.

[43] A. Holmgren, Annu. Thioredoxin, Rev. Biochem. 54 (1985) 237–271.
[44] G. Krause, A. Holmgren, Substitution of the conserved tryptophan 31 in *Escherichia coli* thioredoxin by site-directed mutagenesis and structure-function analysis, J. Biol. Chem. 266 (1991) 4056–4066.
[45] J.F. Collet, J. Messens, Structure function, and mechanism of thioredoxin proteins, Antioxid. Redox Signal. 13 (2010) 1205–1216.
[46] W.D. Comper, in: D.A. Lane, I. Bjoerk, U. Lindahl (Eds.), Heparin Related Polysaccharides, vol. 7, Springer Science & Business Media, Berlin, 1981.
[47] I. Capila, R.J. Linhardt, Heparin-protein interactions, Angew. Chem. Int. Ed. Engl. 41 (2002) 390–412.
[48] T.A. Brown, T.M. Yang, T. Zaitsevskaia, Y. Xia, C.A. Dunn, R.O. Sigle, B. Knudsen, W.G. Carter, Adhesion or plasmin regulates tyrosine phosphorylation of a novel membrane glycoprotein p80/gp140/CUB domain-containing protein 1 in epithelia, J. Biol. Chem. 279 (2004) 14772–14783.
[49] F. Manetti, F. Corelli, M. Botta, Fibroblast growth factors and their inhibitors, Curr. Pharm. Des. 6 (2000) 1897–1924.
[50] A. Garg, S. Garg, L.J.D. Zaneveld, A.K. Singla, Chemistry and pharmacology of the citrus bioflavonoid hesperidin, Phytother. Res. 15 (2001) 655–669.
[51] O. Benavente-Garcia, J. Castillo, Update on uses and properties of citrus flavonoids: new findings in anticancer, cardiovascular, and anti-inflammatory activity, J. Agric. Food Chem. 56 (2008) 6185–6205.
[52] J.A. Manthey, N. Guthrie, K. Grohmann, Biological properties of citrus flavonoids pertaining to cancer and inflammation, Curr. Med. Chem. 8 (2001) 135–153.
[53] J. Yu, L. Wang, R.L. Walzem, E.G. Miller, L.M. Pike, B.S. Patil, BS (2005) Antioxidant activity of citrus limonoids flavonoids, and coumarins, J. Agric. Food Chem. 53 (2005) 2009–2014.
[54] S.L. Hwang, P.H. Shih, G.C. Yen, Neuroprotective effects of citrus flavonoids, J. Agric. Food Chem. 60 (2012) 877–885.
[55] F. Ding, J.X. Diao, Y. Sun, Y. Sun, Bioevaluation of human serum albumin–hesperidin bioconjugate: insight into protein vector function and conformation, J. Agric. Food Chem. 60 (2012) 7218–7228.
[56] A. Ratnaparkhi, S.A. Muthu, S.M. Shiriskar, R.R. Pissurlenkar, S. Choudhary, B. Ahmad, Effects of hesperidin, a flavanone glycoside interaction on the conformation, stability, and aggregation of lysozyme: multispectroscopic and molecular dynamic simulation studies, J. Biomol. Struct. Dyn. 33 (2015) 1866–1879.